Development of a Nanomedicine loaded Hydrogel for Sustained Delivery of an Angiogenic Growth Factor to the Ischaemic Myocardium

Joanne O'Dwyer[1, 2, 3], Robert Murphy[4], Eimear B. Dolan[1, 2], Lenka Kovarova[5, 6], Vladimir Velebny[5], Andreas Heise[4, 7], Garry P. Duffy[2, 3, 7-9], Sally Ann Cryan[1-3, 7-9].

[1]Drug Delivery & Advanced Materials Team & [2]Tissue Engineering Research Group, School of Pharmacy & Dept. of Anatomy, Royal College of Surgeons in Ireland (RCSI)

[3]Trinity Centre for Bioengineering, Trinity College Dublin (TCD)

[4]Department of Pharmaceutical and Medicinal Chemistry, RCSI

[5]R&D Department, Contipro, Dolni Dobrouc 401, 561 02 Dolni Dobrouc, Czech Republic

[6]Brno University of Technology, Faculty of Chemistry, Institute of Physical Chemistry, Purkynova 464/118, 612 00 Brno, Czech Republic

[7]Centre for Research in Medical Devices (CURAM), National University of Ireland Galway (NUIG) & RCSI

[8]Advanced Materials and Bioengineering Research Centre (AMBER), NUIG, RCSI & TCD

[9]Anatomy, School of Medicine, College of Medicine, Nursing and Health Sciences, NUIG

Corresponding author: Prof. Sally Ann Cryan, School of Pharmacy, Royal College of Surgeons in Ireland, 1st Floor, Ardilaun House (Block B), St. Stephen's Green, Dublin 2. Tel: +3531-4022741. Email: scryan@rcsi.ie

Abbreviated title: Nanomedicine-loaded hydrogel for improving cardiac angiogenesis.

Financial support for this project was provided by Science Foundation Ireland under grant number 13/IA/1840 and the AMCARE consortium, a European Union's Seventh Framework Programme (FP7/2007-2013) under grant agreement number 604531.

Abstract

The five year mortality rate for heart failure borders on 50%. The main cause is an ischaemic cardiac event where blood supply to the tissue is lost and cell death occurs. Over time this damage spreads and the heart is no longer able to pump efficiently. Increasing vascularisation of the affected area has been shown to reduce patient symptoms. The growth factors required to do this have short half-lives making development of an efficacious therapy difficult. Herein, the angiogenic growth factor Vascular Endothelial Growth Factor (VEGF) is complexed electrostatically with star-shaped or linear polyglutamic acid (PGA) polypeptides. Optimised PGA-VEGF nanomedicines provide VEGF encapsulation of >99% and facilitate sustained release of VEGF for up to 28 days *in vitro.* The star-PGA-VEGF nanomedicines are loaded into a percutaneous delivery compliant hyaluronic acid hydrogel. Sustained release of VEGF from the composite nano-in-gel system is evident for up to 35 days and the released VEGF has comparable bioactivity to free, fresh VEGF when tested on both Matrigel® and scratch assays. Therefore, we report the development of novel, self-assembling PGA-VEGF nanomedicines and their incorporation into a hyaluronic acid hydrogel that is compatible with medical devices to enable minimally-invasive delivery to the heart. The final star-PGA-VEGF nanomedicine-loaded hydrogel is biocompatible and provides sustained release of bioactive VEGF. This formulation provides the basis for optimal spatiotemporal delivery of an angiogenic growth factor to the ischaemic myocardium.

Keywords: Star polypeptide, nanoparticle, angiogenesis, growth factor, ischaemia.

Introduction

The task of ensuring cell survival in the body resides primarily with the circulatory system [1]. Transport of oxygen and essential nutrients requires an intact and ubiquitous blood vessel network [1, 2]. Blockage of blood vessels, as seen in ischaemic heart disease, causes a reduction in the supply of essential elements to cells in the surrounding area, resulting in cell death and tissue damage [3]. Furthermore, tissue engineering 'scaffolds' are gaining popularity for their use in regenerative medicine but require an adequate blood supply to provide essential elements to the cells at the core of the scaffold and prevent core necrosis [4, 5]. The ability to promote appropriate blood vessel formation therefore has many potential biomedical applications. In cardiac regeneration, the formation of new blood vessels around an infarcted area can reduce cardiomyocyte death and consequently tissue damage [6, 7]. Following myocardial infarction (MI) due to a blocked coronary artery, initial tissue damage is a strong prognostic factor for mortality and progression to heart failure. Interventions that can reduce the area of this damage could form part of a potential treatment for heart failure [3]. Angiogenesis refers to the formation of blood vessels from those already present and agents which can promote angiogenesis offer a possible new treatment modality [8].

It has been almost thirty years since the original discovery of Vascular Endothelial Growth Factor (VEGF) and it has now become known as one of the most potent mediators of angiogenesis [9, 10]. Patients with stable angina have received intracoronary injections of VEGF with the aim of revascularising ischaemic heart tissue. Early clinical trials for that application determined the optimal dose for therapeutic effect and avoidance of side-effects, particularly hypotension [11]. The results of these studies lead on to the VEGF in Ischemia for

Vascular Angiogenesis – 'VIVA' trial where patients received VEGF via intracoronary infusion on day 0, followed by intravenous infusions on days 3, 6 and 9. This clinical trial showed the safety of VEGF therapy. Patients reported improvements in quality of life related parameters and some positive trends in exercise tolerance were observed at day 120 in VEGF treated patients. However, no significant improvement in myocardial perfusion was evident [12]. Resulting from this, it has been established, that to obtain the maximum benefit from VEGF therapy a sustained release of the growth factor at the site of action is required for up to four weeks [13].

This concept of sustained delivery at the site of action or spatiotemporal delivery is often achieved by the delivery of therapeutic molecules in a particulate system. Nanoparticles are preferred for delivery to areas in potential contact with the blood stream particularly for cardiac delivery due to the reduced risk of embolisation [14, 15]. Traditional materials used for VEGF nanoparticle fabrication include poly(L-lactic-*co*-glycolic acid) (PLGA), alginate and dextran-chitosan [16-19]. Oduk et al. recently reported the formation of PLGA-based VEGF nanoparticles which released VEGF for up to 31 days and resulted in significant improvements in infarct size, wall thickness and left ventricular ejection fraction four weeks post myocardial infarction (MI) in a murine model [20]. Other VEGF nanoparticles composed of PLGA or dextran-gelatin have exhibited increases in vessel density and tissue perfusion in pre-clinical *in vivo* studies [17, 18]. However, translation to the clinic has been slow with no VEGF particulate system licensed to-date. Barriers to clinical and commercial translation of VEGF-loaded nanomedicines include issues with the nanoparticle fabrication process such as difficulty in scaling-up and inadequate protein encapsulation and loading [21]. Thus, an unmet

clinical need exists regarding materials which can produce sustained release nanomedicines using a scalable and efficient manufacturing procedure.

Electrostatic interaction is a technique commonly used for the formation of nucleic acid containing nanoparticles but its use in the formation of protein loaded nanoparticles is still in its infancy. Electrostatic complexation of two oppositely charged molecules is a relatively simple process that reduces the potential for protein damage and is amenable to scale-up. Yan et al. previously reported the successful incorporation of insulin, via electrostatic interaction, into a star-shaped poly(L-lysine) (PLL) polypeptide delivery system [22]. The particles produced by Yan et al. exhibited sustained, pH responsive insulin release *in vitro*. Creating a similar system with VEGF may result in the ability to sustain its release [22]. Unlike insulin, VEGF is positively charged at physiological pH and thus a negatively charged polypeptide would be required to facilitate electrostatic interaction. Byrne et al. have previously reported the synthesis of negatively charged glutamic acid (PGA) polypeptides with both a star-shaped and linear geometry [23]. Due to their higher molecular weight star-shaped polypeptides have more binding sites than their linear counterparts allowing greater interaction with the therapeutic cargo at a lower dose [23]. Yan et al. also reported an encapsulation efficiency of almost 100% in their work. This has advantages in terms of the cost of nanomedicine manufacture. PGA polypeptides could therefore facilitate electrostatic interaction with the positively charged sites on VEGF to prepare the sustained release nanomedicines.

Maintaining the VEGF nanomedicines at the site of action is critical to their effectiveness; such approaches could be optimised by utilising biomaterials, specifically hydrogels, as delivery vehicles to enhance retention at the desired site. Hydrogels are particularly suitable for

cardiac applications due to their biocompatibility, potential for minimally invasive delivery and mechanical properties [24-26]. An alginate hydrogel-Algisyl® (LoneStar Heart, Inc., USA) is currently in clinical trials. Following implantation into the heart wall Algisyl® improves the strength of the wall, the heart's ability to pump and the patient's symptoms (27).

In light of its advantageous biocompatibility and physicochemical properties, hyaluronic acid (HA) was chosen to act as the nanoparticle delivery vehicle in this case [28]. HA is a naturally occurring polysaccharide. Native HA is rapidly degraded by hyaluronidases *in vivo*. Various types of modified HA molecules have been produced to overcome this rapid breakdown and to improve the mechanical properties of HA [28]. With a view to cardiac application of this system, we loaded the PGA-VEGF nanomedicines into a tyramine modified hyaluronic acid hydrogel (HA-TA) to further sustain the VEGF release and maintain the nanomedicines at the site of action. Overall then, we aimed to develop a nano-in-gel system suitable for the delivery of VEGF in a spatiotemporally controlled manner to the myocardium.

Methods

Materials

Recombinant Human $VEGF_{165}$ and the Human VEGF Quantikine ELISA kits used were obtained from R&D Systems (UK). Illustra MicroSpin S-400 HR columns were purchased from GE Healthcare (UK). Float-A-Lyzers were obtained from Spectrum Labs (UK). EndoGrow cell culture medium was purchased from Merck Millipore Ltd. (Ireland). Growth factor reduced Matrigel® was purchased from Corning BV (Netherlands). Human umbilical vein endothelial cells (HUVECs) were obtained from Lonza Ltd (UK). All other chemicals and reagents were sourced from Sigma Aldrich (Ireland). Star polypeptides were made following a protocol previously developed by Byrne et al. [23].

Preparation of VEGF-loaded nanomedicines

Two glutamic acid polypeptides linear polyglutamic acid (L-PGA) and star-shaped polyglutamic acid (star-PGA) were synthesised. A series of formulations were prepared with differing PGA:VEGF ratios. Herein we will focus on three formulations linear PGA:VEGF 30:1 (L-PGA-VEGF 30:1), star-PGA:VEGF 30:1 (star-PGA-VEGF 30:1) and star-PGA:VEGF 50:1 (star-PGA-VEGF 50:1). The ratios stated represent molar ratios of star-PGA to VEGF based on their relative molecular weights. In the case of the L-PGA-VEGF formulation the 30:1 ratio has the same number of glutamic acid units per molecule of VEGF as the star-PGA-VEGF 30:1 ratio. Nanoparticle fabrication was achieved using a self-assembly technique. Phosphate Buffered Saline (PBS), pH 7.4 was first added to an eppendorf, star-PGA or L-PGA was then added, depending on the formulation. Finally, VEGF was added and the preparation was allowed to complex. Four different complexation conditions were trialled: 5 minutes at room temperature, 5 minutes in the fridge, 30 minutes at room temperature and 30 minutes in the fridge.

Characterisation of PGA-VEGF nanomedicines

Particle size and Zeta potential

Z-average size of the L-PGA-VEGF and star-PGA-VEGF formulations was investigated using Dynamic Light Scattering (DLS). Preparations were made as described above, to a volume of 50 µl, following complexation for five minutes at room temperature, molecular grade water was added to a final volume of 1 ml and the resulting dispersion was placed in a Zetasizer Nano ZS (Malvern Instruments, UK). Particle size was determined using a 100 mW laser beam at a backscatter angle of 173°. All measurements were performed at 25°C and samples were allowed to equilibrate in the machine for two minutes before measurement commenced. Polydispersity Index (PDI) for each of the samples was recorded to assess the particle size distribution. The Zeta potential of the nanoparticles was also assessed on a Zetasizer Nano ZS, using the same preparation procedure as for size measurement.

Nanotracking Analysis (NTA) was used to further evaluate particle size. NTA was performed on a Nanosight NS 300 (Malvern Instruments, UK). Dispersions were made to a 50 µl volume and diluted with molecular grade water to 1 ml for analysis. The sample was then injected through a flow through cell using the automated injection system on the machine. Thermoelectric Peltier elements on the machine allowed for temperature control at 22°C during sample measurement. Real-time images were obtained for sixty seconds and this 'video' was then analysed using a suitable particle detection threshold.

Encapsulation efficiency and protein loading capacity

Illustra MicroSpin S-400 HR columns were employed to determine the amount of protein complexed to the PGA, with intact VEGF nanomedicines retained on the column and non-encapsulated VEGF eluted. Columns were prepared following the manufacturer's instructions and 100 µl of each of the nanoparticle dispersions was added to the spin column, followed by centrifugation in a VWR Galaxy 14D microcentrifuge at 700 x g for two minutes. The eluted liquid was removed and stored at -80°C for later analysis. Encapsulation efficiency was calculated using the following equation:

Encapsulation Efficiency (%) =

$$\frac{(\quad) - (\quad)}{(\quad)} \times 100$$

The loading capacity of the PGA-VEGF nanomedicines was calculated taking into account the encapsulation efficiency. The loading capacity was calculated using the following equation:

Loading Capacity (%) =

$$\frac{(\quad)}{(\quad)} \times 100$$

***In vitro* drug release studies**

A 1 ml cellulose ester membrane Spectra/Por® Float-A-Lyzer® G2 device with a molecular weight cut-off (MWCO) of 300 kDa which allowed the protein to pass through but retained the intact nanoparticles was used to perform these studies. Nanoparticle dispersions containing 50 ng VEGF were placed in the centre of the Float-A-Lyzer® which was then put in 5 ml of release medium (PBS) in the receptor fluid container. The Float-A-Lyzer® container combination was then placed in a 50 ml Falcon tube and put in a water bath at 37°C shaking at a rate of 75 rpm. Release medium was removed entirely and new, pre-warmed medium

was added at each time point. Time points were taken at 2, 4, 6, 8 hours and on days 2, 3, 4, 5, 7, 14, 21, 28 and 35. Release medium was frozen at -80°C for analysis at a later time. Release samples were analysed via ELISA which was carried out exactly according to the manufacturer's instructions. Quantification of VEGF was determined by measuring absorbance on a Varioskan plate reader at 450 nm with correction at 570 nm.

***In vitro* bioactivity of PGA-VEGF nanomedicines**

Culture of human umbilical vein endothelial cells (HUVECs)

Following revival, HUVECs were cultured in T75 flasks at 37°C and 5% CO_2. HUVECs were seeded at a density of 1 x 10^6 cells per flask and were passaged when they reached 80% confluency. HUVECs were fed with EndoGrow medium containing all required growth supplements (rhVEGF 5 ng/ml, rhEGF 5 ng/ml, rhFGF 5 ng/ml, rhIGF-1 15 ng/ml, Ascorbic Acid 50 µg/ml, Hydrocortisone Hemisuccinate 1 µg/ml, Heparin Sulphate 0.75 U/ml, L-Glutamine 10 mM, Foetal Bovine Serum (FBS) 2% and Penicillin/Streptomycin 1%). VEGF was used at a concentration of 5 ng/ml for feeding the cells during expansion but was removed, in all cases for cell studies. Biocompatibility testing was carried out initially and the methods and results are included in the supplementary material.

Tubule formation-Matrigel® assay

In vitro microvessel/tubule formation assays can be used as an indicator of potential *in vivo* angiogenic activity [29-31]. 120 µl of growth factor reduced, phenol red free Matrigel® was placed in each well of a 48 well plate and incubated at 37°C for 30 minutes. HUVECs were seeded on top of the Matrigel® at a density of 3 x 10^4 cells per well in a spiral pattern [32]. Control groups consisted of endothelial growth medium with no VEGF or endothelial growth

medium with 50 ng/ml non-encapsulated VEGF. Three nanomedicine treatment groups were used: L-PGA-VEGF 30:1, star-PGA-VEGF 30:1 and star-PGA-VEGF 50:1. Each nanomedicine formulation contained 50 ng VEGF. Nanomedicines were added directly to the culture medium. Tubule formation was assessed by taking five photographs of each well using a Leica Microscope (Leica Microsystems, Switzerland) at 10X magnification at 6, 12 and 24 hours. Total tubule length was determined by finding the sum of the tubule lengths per well using ImageJ software (National Institutes of Health).

Cell migration-Scratch assay

HUVECs were seeded on a 24 well plate at a seeding density of 3×10^4 cells per well and fed with complete endothelial medium until a confluent monolayer of cells was present in the plate. At this point medium was removed from all wells and a P200 pipette tip was used to scratch a vertical line down through the cell monolayer thus removing the cells in this location. Each of the wells was washed three times with 500 µl PBS to remove the detached cells. Treatments and controls were then added to the wells. FBS was removed from the medium for this experiment to reduce the potential for cell proliferation interfering with results. Wells were imaged at 5X magnification at time zero and the position of the image marked on the plate to ensure consistency of imaging throughout the experiment. Images were taken at 0, 6, 12 and 24 hours. Gap distance was measured in three locations on the image using ImageJ software.

Fabrication and characterisation of PGA-VEGF nanomedicine-loaded hyaluronic acid hydrogels

Tyramine-modified hyaluronic acid (HA-TA) (250-350 kDa) was kindly provided by Contipro (Czech Republic). Hydrogel formation involved dissolving the HA-TA in PBS at the relevant concentration, taking account of the volume of nanoparticles to be added. The resulting dispersion was placed on a roller-plate overnight to ensure complete wetting of the freeze-dried HA-TA powder. Following this the HA-TA dispersion was divided into two separate Falcon tubes. The final concentration was adjusted by addition of the nanoparticle dispersion to one tube and PBS to the other to ensure both contained the same concentration of HA-TA in either PBS alone or a PBS/nanoparticle containing solution. Horseradish peroxidase (HRP) was added to one Falcon tube at a concentration of 0.24 U/ml and Hydrogen peroxide (H_2O_2)

was added to the other tube at 0.88 µmol/ml. These agents acted as the crosslinkers required for gelation to occur. It was imperative to keep the crosslinkers separated until gelation was required, thus the dispersions from each Falcon tube were drawn up into two separate 1 ml syringes. These were then attached to a benchtop hydrogel mixer (BHM) (Fig. 1(b)) (Contipro, Czech Republic) which contained a static mixer to facilitate correct interaction of the components on injection to allow gelation. This system is shown in Fig. 1.

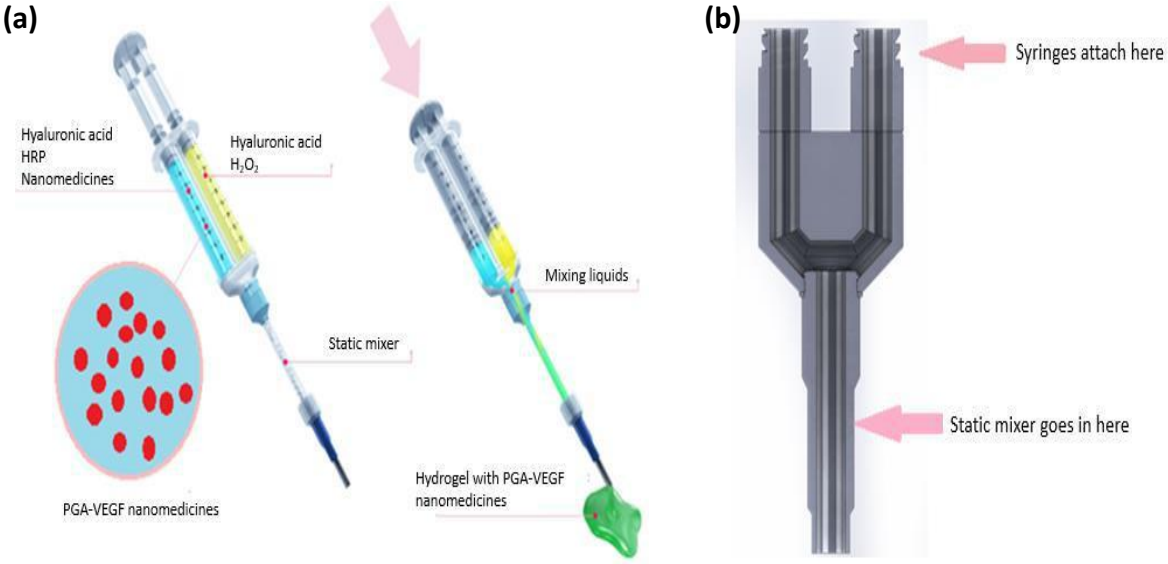

Fig. 1(a) System used to formulate the nanomedicine-loaded hyaluronic acid hydrogel, showing addition of Horseradish peroxidase and PGA-VEGF nanomedicines to one syringe and hydrogen peroxide to the other syringe. Preparations then pass through the benchtop hydrogel mixer device **(b)** where the static mixer produces homongeous mixing of the two components to form a hydrogel.

Rheological testing

Rheology was performed on an AR-1000 cone and plate rheometer (TA Instruments, USA). Time sweeps were performed at 21°C, under a shear stress of 5 Pa and frequency of 1 Hz for thirty minutes.

Hydrogel homogeneity

Assessment of particle distribution in the hydrogel was achieved by fluorescently tagging the star-PGA polypeptide using an Alexa Fluor™ 488 Microscale Protein Labeling Kit. Tagging was performed using the kit as per the manufacturer's guidelines. The final product was centrifuged to remove any residual unbound tag and a standard curve was produced to facilitate concentration determination. This fluorescent tag was capable of binding to a primary amine group of the PGA polypeptide, without interfering with VEGF binding. Star-PGA-VEGF 50:1 nanomedicines were then formulated using this fluorescently tagged PGA and incorporated into the hydrogel as previously described. A confocal microscope (Carl Zeiss, Germany) was used to visualise the dispersion of nanoparticles in the hydrogel.

Analysis of VEGF release and bioactivity from the nanomedicine-loaded hydrogel

A 200 µl cylinder of gel was placed inside a 1 ml cellulose ester membrane Spectra/Por® Float-A-Lyzer® G2 device with a MWCO of 300 kDa and a further 200 µl of PBS was placed on top of the hydrogel sample. The release study then proceeded as described in the '*In vitro* drug release studies' section described above, with VEGF detection again being performed via

ELISA. To ensure the bioactivity of the released VEGF, the release supernatant from all time points up to day 14 was pooled, concentrated using an Amicon® Ultra 15 ml centrifugal filter with a molecular weight cut-off of 3 kDa and the concentrated solution was applied to both a Matrigel® and a scratch assay which again were carried out as described above.

Statistical analysis

All statistical tests were performed using GraphPad Prism v5 (GraphPad Software Inc., CA, USA). Mean and standard error of the mean are presented on all graphs. A one-way ANOVA followed by Bonferroni post-hoc test was used to analyse the data obtained from the Matrigel® and scratch assays. Significance was determined as $p<0.05$. Three repeats were performed for all experiments.

Results

Synthesis of glutamic acid–based polypeptides

L-PGA contained 200 glutamic acid residues per molecule (Mn: 26 kDa) (Fig. 2(a)). The star-shaped PGA had a polypropyleneimine (PPI) core and eight arms, each with 40 glutamic acid residues (theoretical Mn: 42 kDa; estimated isoelectric point: 4.1). The structure of this star-PGA is shown in Fig. 2(b). Gel permeation chromatograms for both L-poly-γ-benzyl-L-

glutamate (PBLG) and star PBLG, the precursors to L-PGA and star-PGA are shown in Online Resource 1.

(a) **(b)**

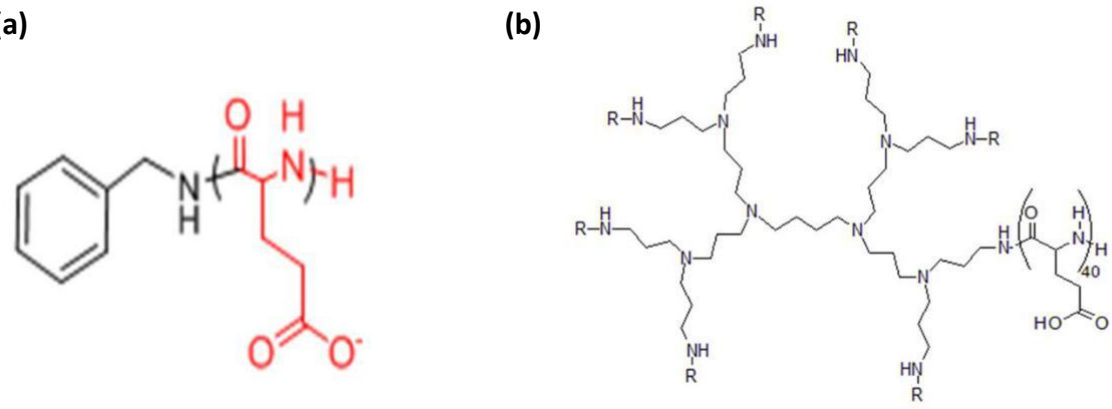

Fig. 2(a) The linear PGA and **(b)** star-PGA polypeptides synthesised which will be used for nanomedicine fabrication in this work.

Characterisation of PGA-VEGF formulations

Particle formulation

Particle dispersions were formed by adding star-PGA or L-PGA to an eppendorf followed by the requisite amount of VEGF and PBS to a final volume of 50 µl. Seven different molar ratios of star-PGA:VEGF were initially trialled based on a star-PGA molecular weight of 42 kDa and a VEGF molecular weight of 42 kDa. Four complexation procedures were used: 5 minutes complexation at room temperature, 30 minutes complexation at room temperature (~21°C) and either 5 or 30 minutes complexation in the fridge (2-8°C). The results from these initial studies are shown in Online Resource 2. Based on the particle sizes shown in Online Resource 2, 5 minutes complexation at room temperature was chosen as the optimal complexation technique because this procedure produced nano-sized particles while also being appropriate for translation of manufacture to a larger scale. L-PGA-VEGF formulations were complexed

for 5 minutes at room temperature. As stated previously, in this paper we will focus on three formulations L-PGA-VEGF 30:1, star-PGA-VEGF 30:1 and starPGA-VEGF 50:1, the rationale for choosing these formulations is discussed in Online Resource 2.

Particle size and Zeta potential

As shown in Table 1, DLS indicated the formation of nano-sized particles for L-PGA-VEGF 30:1 and star-PGA-VEGF 30:1 and 50:1 formulations. Of these three formulations L-PGA-VEGF was the largest with a Z-average size of 656.7 nm. The star-PGA-VEGF 30:1 and 50:1 formulations were very similar in size with Z-averages of 444.5 nm and 415.5 nm respectively. The Zeta potential data demonstrated a negative surface charge for all formulations. This charge was very close to neutral for the star-PGA-VEGF 30:1 and 50:1 formulations at -2.3 meV and -3.6 meV respectively. The Zeta potential of the L-PGA-VEGF 30:1 formulation was slightly more negative than that of the star-PGA-VEGF formulations at -7.7 meV. Particle size measurements on the Nanosight, 203 nm for star-PGA-VEGF 30:1 and 196.4 nm for star-PGA-VEGF 50:1, indicated smaller sizes than those observed with DLS for star-PGA-VEGF nanoparticles. However, similar to the DLS data the size of star-PGA-VEGF 30:1 was similar to that of star-PGA-VEGF 50:1. L-PGA-VEGF formulations could not be observed on the Nanosight. Encapsulation efficiency for all formulations was greater than 99.99% w/w indicating almost complete encapsulation of the VEGF. Loading capacity varied from 2% w/w to 3.33% w/w (50 ng/1.5 μg to 50 ng/2.5 μg) depending on the molar ratio of PGA to VEGF used.

Table 1 Physicochemical characterisation of PGA-VEGF formulations (n=3). No particles were detected for L-PGA-VEGF 30:1.

Formulation	Z-average size (nm)	Zeta Potential (meV)	Polydispersity Index	Average size Nanotracking Analysis (nm)	Encapsulation Efficiency	Loading Capacity (% w/w)
L-PGA-VEGF 30:1	656.7	-7.7	0.4		>99.9%	3.33%
Star-PGA-VEGF 30:1	444.5	-2.3	0.3	203	>99.9%	3.33%
Star-PGA-VEGF 50:1	415.5	-3.6	0.2	196.4	>99.9%	2%

***In vitro* release of VEGF from PGA-VEGF nanomedicines**

Following confirmation of nanomedicine formation and VEGF encapsulation, the rate of VEGF release from the nanomedicines was determined. Results are shown as the cumulative percentage of VEGF originally encapsulated released up to and including the relevant time

point. As shown in Fig. 3 L-PGA-VEGF formulations exhibited more rapid release with 30% of the loaded VEGF released at day 7, compared to 17% and 18% release from the star-PGA-VEGF 30:1 and 50:1 formulations respectively. No release was detected from this L-PGA-VEGF formulation after day 7. In contrast the two star-PGA-VEGF formulations released VEGF for 28 days, with no release detected thereafter. There was no significant difference between the two star-PGA formulations, in terms of release at any time point.

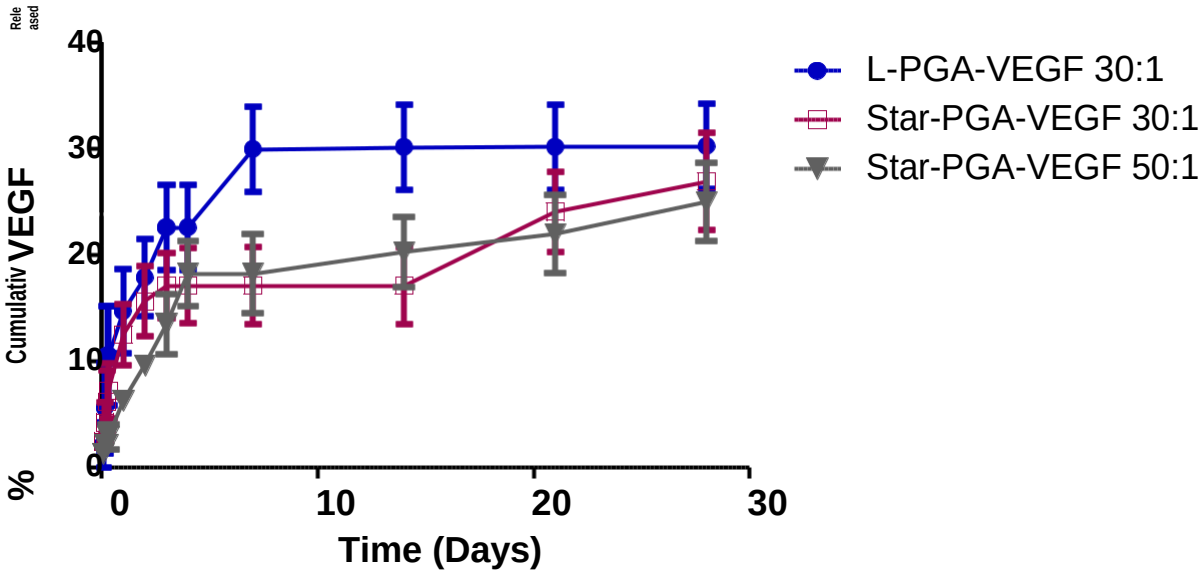

Fig. 3 Cumulative percentage VEGF released from L-PGA-VEGF or star-PGA-VEGF formulations over 28 days. The star-PGA-VEGF formulations exhibited more sustained VEGF release than the L-PGA-VEGF formulation. All formulations contained 50 ng VEGF. n=3.

Bioactivity of PGA-VEGF nanomedicines: tubule formation

The bioactivity of the PGA-VEGF nanomedicines was next assessed by investigating their ability to induce microvessel/tubule formation *in vitro*. Total tubule length was measured here as this was deemed to be the most appropriate parameter for this application. Linear and star-PGA-VEGF (50 ng VEGF) nanomedicine formulations are compared to controls of

untreated cells (cells alone) and cells exposed to fresh, non-encapsulated VEGF at a comparative dose of 50 ng. Fig. 4(a) shows that, overall, much better interlinked microvessel networks are present in groups treated with VEGF. As presented in Fig. 4(b) star-PGA-VEGF 30:1 and 50:1 formulations were capable of inducing the same degree of tubule formation at 6 hours as non-encapsulated VEGF and all treatment groups significantly increased total tubule length compared to cells alone. At 12 hours, star-PGA-VEGF 30:1 and 50:1 were again significantly better than cells alone. In contrast, the L-PGA-VEGF nanomedicines were not significantly better than cells alone at 6 hours. The L-PGA formulation did exhibit a significant increase in tubule length over cells alone at 12 hours, although less than the increase observed for the star-PGA-equivalents. At 24 hours, tubule regression is occurring in all groups and tubule length is reduced. This is considered to be the typical behaviour of such structures in this assay [32].

(a) (i) (ii) (iii)

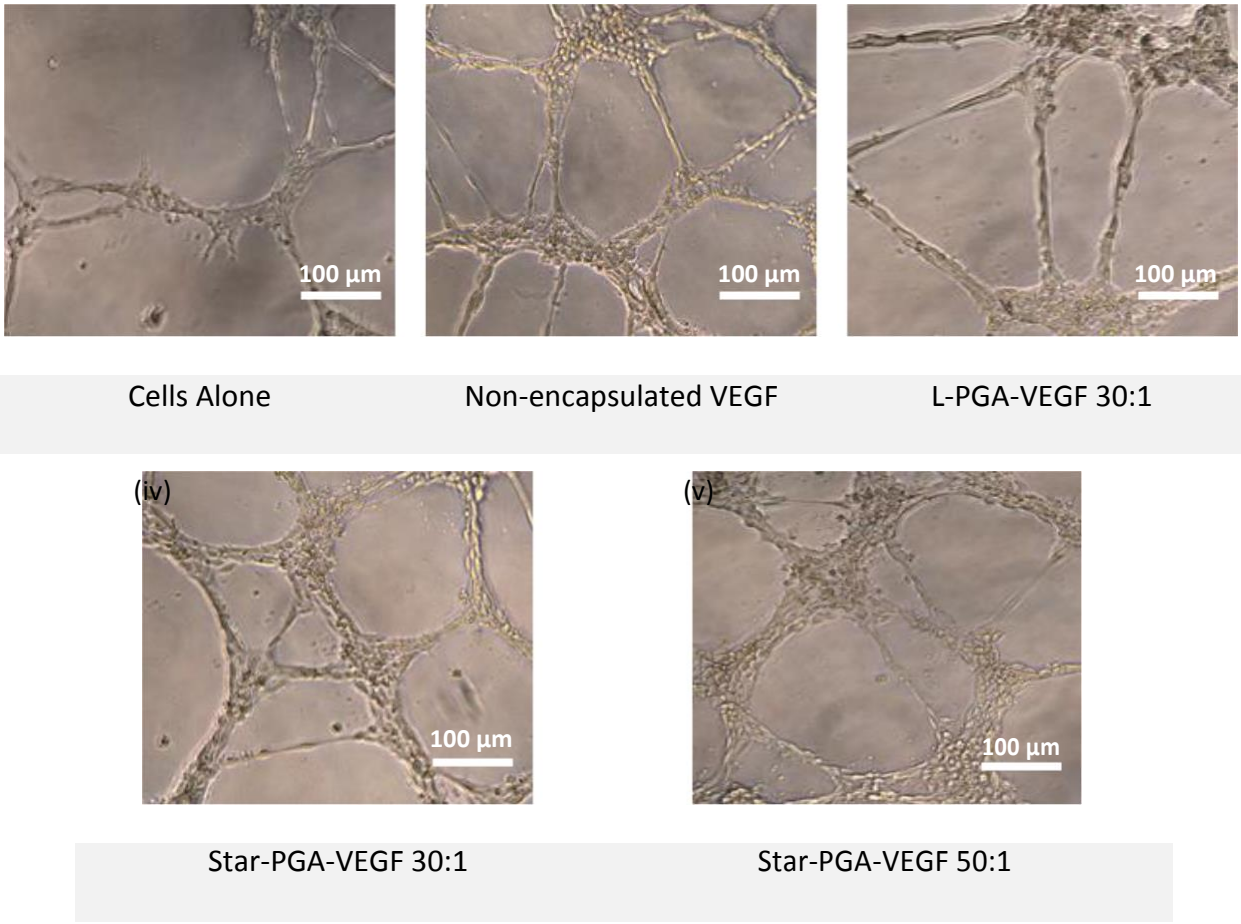

(b)

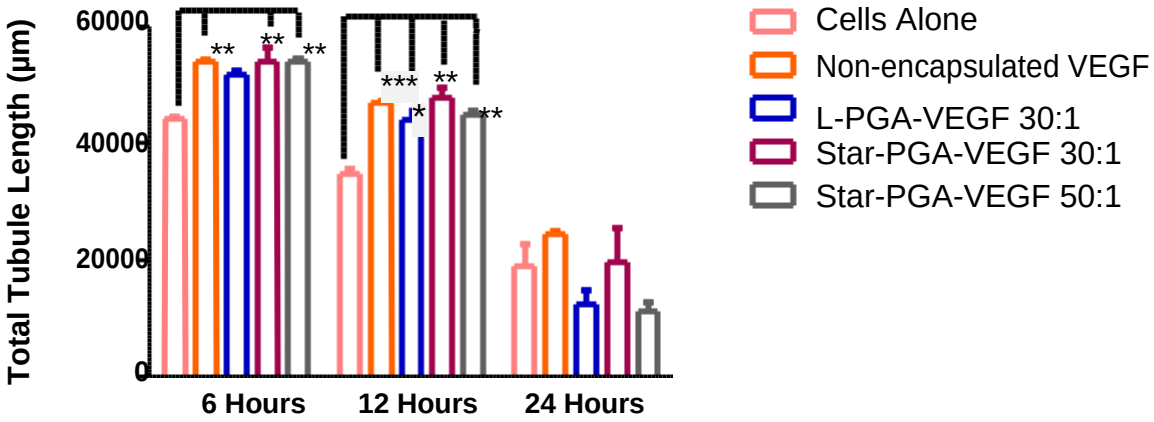

Fig. 4 Bioactivity of VEGF released from PGA-VEGF nanoparticles **(a)** Microscopy images of tubule formation following 12 hours of culture. All groups display better tubule formation than the cells alone group not exposed to VEGF. **(b)** Quantification of tubule lengths at 6, 12 and 24 hours, confirming significantly better tubule lengths with all VEGF containing groups at 12 hours. All formulations contained 50 ng VEGF. n=3; *p<0.05, **p<0.01, ***p<0.001.

Bioactivity of PGA-VEGF nanomedicines-cell migration

Cell migration is also a key process in *in vivo* angiogenesis and therefore the efficacy of the VEGF formulations was investigated using a scratch assay. 6 hours following gap formation and treatment addition, non-encapsulated VEGF treatment had led to a significant reduction in the gap width, but no significant reduction was seen for the other treatment groups (Fig. 5(b)). At 12 hours the gap width was 23% of the original width in the non-encapsulated VEGF group and 20% of the original width in the star-PGA-VEGF 50:1 nanomedicine treated group. Both of these groups, non-encapsulated VEGF and star-PGA-VEGF 50:1 had significantly reduced the gap width compared to cells alone (gap width 53% of original width). Both non-encapsulated VEGF and star-PGA-VEGF 50:1 effected closure of the gap by 24 hours while cells alone, L-PGA-VEGF 30:1 or star-PGA-VEGF 30:1 nanomedicines did not achieve gap closure at 24 hours.

(a)

(i) (ii) (iii)

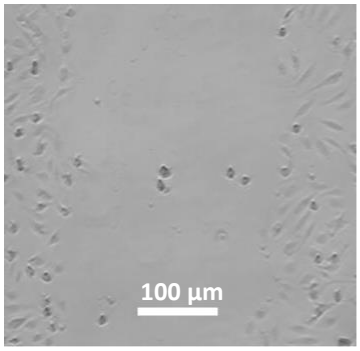

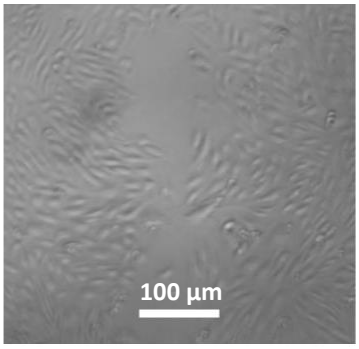

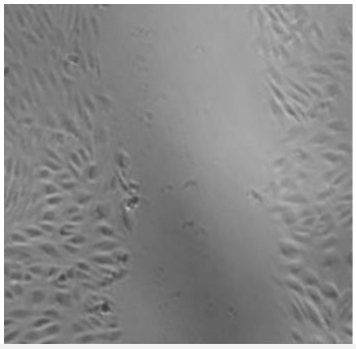

Cells Alone | Non-encapsulated VEGF | L-PGA-VEGF 30:1

(iv)

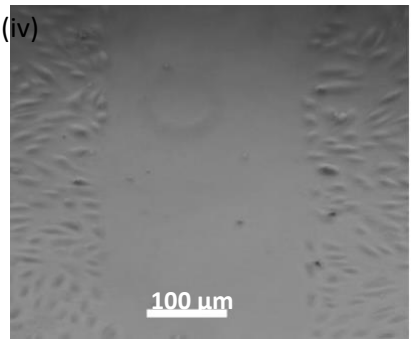

(v)

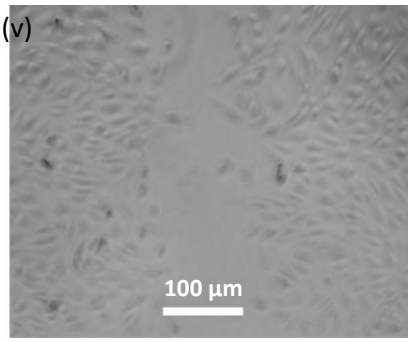

Star-PGA-VEGF 30:1 | Star-PGA-VEGF 50:1

(b)

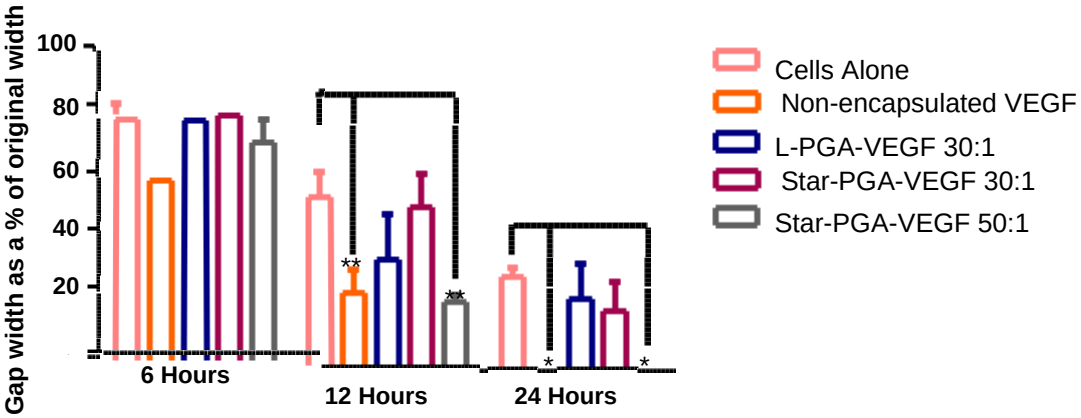

Fig. 5 Cell migration assessed via gap closure achieved on a scratch assay **(a)** Microscopy images of the gap area 12 hours following addition of treatments. **(b)** Quantification of gap closure showing the star-PGA-VEGF 50:1 formulation closing the formed gap as efficiently as the non-encapsulated VEGF. Where VEGF is present the concentration is 50 ng/ml. n=3; *p<0.05, **p<0.01.

Incorporation of star-PGA-VEGF 50:1 nanomedicines into a HA-TA hydrogel

Star-PGA-VEGF 50:1 nanomedicines, which had produced significant results in both Matrigel® and scratch assays, were incorporated into a HA-TA polymer dispersion as described. Rheology was performed on the formulation following transit through the benchtop hydrogel mixer (BHM), as shown in Fig. 1, to assess the effect of nanomedicine incorporation on hydrogel formation. Hydrogel formation is indicated when the storage modulus (G') exceeds the loss modulus (G''). Fig. 6(a) shows that despite the addition of the nanomedicines to the HA-TA dispersion, gelation still occurred and equilibration of storage modulus was achieved more rapidly than with the HA-TA formulation alone. Overall, storage modulus was reduced in the presence of the star-PGA-VEGF 50:1 nanomedicines. Fig. 6(b) shows the dispersion of the fluorescently tagged star-PGA-VEGF nanomedicines in a circular section of the hydrogel, confirming their ability to travel through the BHM and their homogenous distribution in the resulting hydrogel.

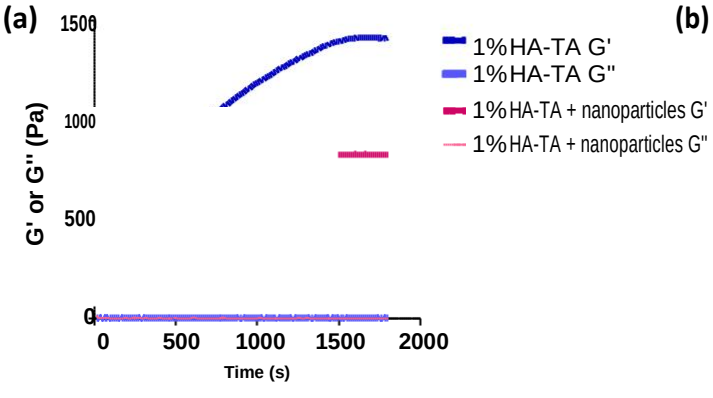

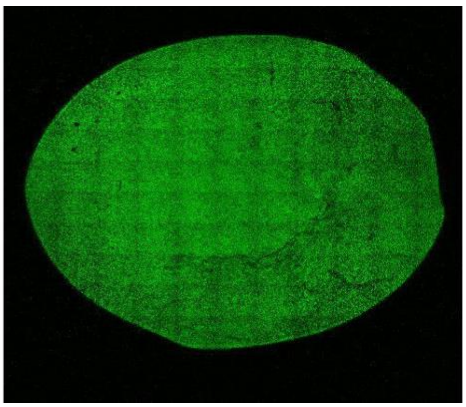

Fig. 6 (a) Rheogram obtained from a thirty minute time sweep showing storage (G') and loss (G'') modulus of the HA-TA gel with or without star-PGA-VEGF 50:1 nanomedicines. Gel formation occurs even in the presence of the nanomedicines. **(b)** Dispersion of fluorescently tagged star-PGA-VEGF 50:1 nanomedicines in the HA-TA hydrogel. VEGF concentration is 50 ng per 200 µl hydrogel portion.

VEGF release and bioactivity of the star-PGA-VEGF nano-in gel system

Free VEGF and PGA-VEGF nanomedicines were both loaded into separate HA-TA hydrogels and VEGF release and the bioactivity of released VEGF determined. Free VEGF was rapidly released from the HA-TA hydrogel with 17.3% of the loaded VEGF released by 24 hours (Fig. 7(a)). No further VEGF release was detected from the hydrogel system for this formulation. Where VEGF was incorporated into the gel as a PGA-VEGF nanomedicine, only 2.86% of the VEGF was released at 24 hours, with release continuing to be detected for up to 35 days. Loading star-PGA-VEGF 50:1 nanomedicines in the HA-TA hydrogel increased VEGF recovery to 45% compared to a recovery of just 17% when free VEGF was loaded into the HA-TA hydrogels. At the end of the experiment, all hydrogels were degraded with hyaluronidase and the resulting liquid was applied to an ELISA. No VEGF was found in these degraded hydrogels (data not shown).

To confirm that the bioactivity of the released VEGF was not affected by the hydrogel fabrication process Matrigel® and scratch assays were carried out using the pooled, concentrated VEGF collected from the release supernatants. Fig. 7 (b) and (c) show that VEGF released from both gel systems was capable of producing tubule lengths analogous to those produced by the control treatment of a comparative dose of non-encapsulated, fresh VEGF. Furthermore, VEGF released from the PGA-VEGF-HA-TA system significantly improved total tubule length at the 6 hour timepoint compared to cells alone. This retained bioactivity of

released VEGF was also evidenced in the scratch assay where gap closure produced by the VEGF released from the star-PGA-VEGF 50:1 loaded HA-TA gel was similar to that produced by the same dose of fresh, free VEGF. There was no significant difference in effect between the VEGF released from the free VEGF loaded into HA-TA and star-PGA-VEGF loaded HA-TA.

(a)

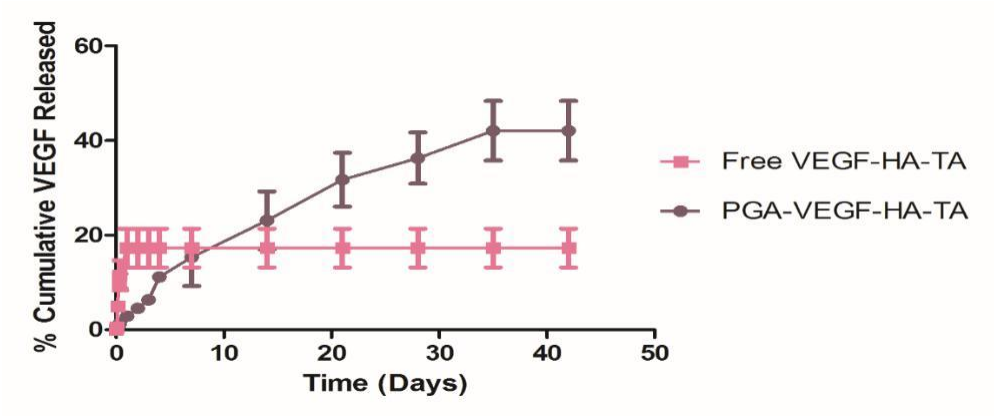

(b)

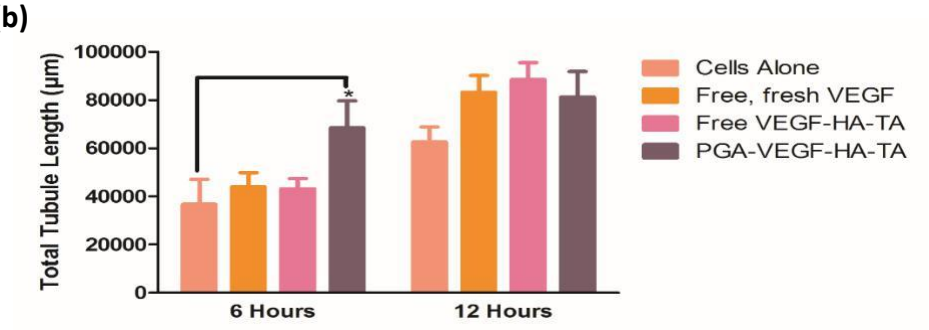

(c)

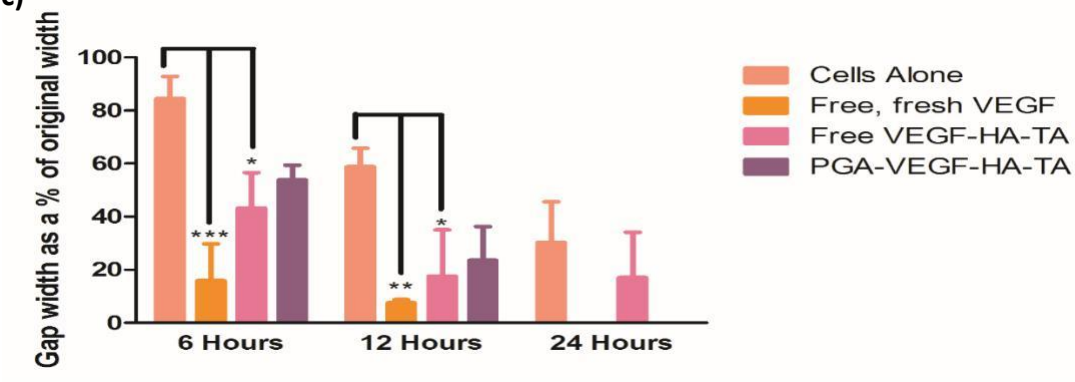

Fig. 7 (a) VEGF released from HA-TA hydrogels either with or without initial incorporation into a nanoparticle. Nanoparticle encapsulated VEGF exhibited more sustained release from the hydrogel than non-encapsulated VEGF. **(b)** Total length of tubules recorded in response to VEGF released from hydrogels with non-encapsulated VEGF used as a bioactivity control. The total tubule length produced in response to the VEGF released from HA-TA hydrogels is in the

same range as that induced by fresh, non-encapsulated VEGF. **(c)** Gap closure on a scratch assay again indicating that VEGF released from HA-TA hydrogels is bioactive. Fresh, free VEGF: 10 ng/ml, Free VEGF-HA-TA: 8.65 ng/ml, PGA-VEGF-HA-TA: 11.5 ng/ml. n=3; *p<0.05, **p<0.01, ***p<0.001.

Discussion

One of the main issues hindering the exploitation of growth factors as therapeutics for biomedical applications is their rapid degradation *in vivo* [33, 34]. The angiogenic growth factor VEGF has been proposed to be useful for applications where improved blood supply to a target tissue is required. Herein a novel approach to improve the stability and control the release of VEGF, using an oppositely charged polypeptide-based carrier, was investigated. This carrier is biocompatible and employs a non-destructive manufacturing process, amenable to scale-up for loading the VEGF. These VEGF nanomedicines were loaded into a hyaluronic acid hydrogel similar to one which has previously shown promise for its ability to improve outcomes post-MI in animal models [35].

Negatively charged PGA polypeptides with either a star-shaped or linear architecture were synthesised to bind electrostatically to the positively charged site on VEGF. Neither of these polypeptides have, to the best of our knowledge, previously been investigated for their ability to complex with VEGF. Both the linear and star-shaped architectures were trialled as such differences in polymer architecture have previously been shown to alter binding capabilities with therapeutics and *in vivo* half-life of nanomedicines [36]. Two star-PGA based formulations were used to assess if different molar ratios affected particle formation and/or activity and an L-PGA-VEGF 30:1 nanomedicine formulation was used as a direct comparator to the star-PGA-VEGF 30:1 formulation again to assess differences in particle characteristics when formed with different polypeptide architectures.

Nanoparticles are an attractive modality for controlled release in cardiac applications with a lower potential for embolization than microparticles [14, 15]. No optimal criteria for nanoparticle delivery to the heart have been established but previous publications have had some success in *in vivo* studies with particles ranging from 115 nm to 400 nm, which efficiently delivered the loaded growth factor and did not produce any adverse events [16, 18, 20].

Both L-PGA-VEGF and star-PGA-VEGF formulations produced nanomedicines with a low PDI on DLS measurements with slightly negative surface charges which was expected given the excess of PGA in the formulations. Star-PGA-VEGF 30:1 and 50:1 formulations were approximately 400 nm when measured using DLS but only 200 nm when measured by NTA. This phenomenon is not unusual and has been reported in the literature as being due to the differing modes of operation of the two instruments [37, 38]. The size of the star-PGA-VEGF 30:1 and 50:1 nanomedicines exceeds that of 50 nm observed by Yan et al formulating insulin nanoparticles with a star PLL-Poly(ethylene glycol) (PEG) polypeptide using a similar procedure [22]. This disparity may be due to the large difference in size between VEGF (42 kDa) and insulin (5 kDa). Star PLL-based formulations used to encapsulate plasmid DNA have previously been shown to be in the range of 140 nm [39].

L-PGA-VEGF nanomedicines were not evident when using the NTA. This may indicate inferior VEGF binding in the L-PGA-VEGF formulations. It has previously been shown that *in vivo* the half-life of L-PGA is 13 times shorter than a star-shaped comparator and this may have an impact on particle stability even *in vitro* [36]. Furthermore, nanomedicines formed from star

polypeptides may have a more globular shape than their linear counterparts which may also explain why detection using NTA which is optimised for globular systems is more difficult [36].

Kita et al. have suggested that optimising encapsulation efficiency should be the top priority in the development of drug delivery systems and an encapsulation efficiency of >99.9% was achieved for all PGA-VEGF formulations tested, both linear and star-shaped [41]. Encapsulation efficiencies for VEGF-loaded nanoparticles reported in the literature vary greatly from 53.5% for PLGA-based nanoparticles synthesised by Oduk et al, to 76% as reported by des Rieux et al. for dextran-chitosan-based nanoparticles [18, 20]. The encapsulation efficiency obtained in this study for PGA-VEGF nanoparticles mirrors that obtained by Yan et al. for insulin encapsulation in their star PLL-PEG system which was reported as "*almost 100%*"[22]. The maximum loading capacity feasible in this system was 3.33% w/w (50 ng/1.5 µg). Again this was similar to the star PLL-insulin nanoparticles formulated by Yan et al, who reported a maximum loading capacity of 4.9% [22]. Golub et al., Oduk et al. and des Rieux et al. reported loading capacities of 5.3%, 0.01% and 0.5% respectively when loading VEGF into more traditional PLGA (5.3 and 0.01%) or dextran-chitosan-based (0.5%) nanoparticles [16, 18, 20]. The high encapsulation efficiency and ease of loading is a significant advantage of this PGA formulation, preventing loss of expensive therapeutic protein during nanoparticle fabrication, a major translational hurdle.

Prolonged release of VEGF is required to facilitate optimal vessel growth [13, 41]. Star-PGA-VEGF 50:1 nanomedicines released 72% of the total released VEGF by day 7 with further release observed until day 28. In contrast, VEGF release from the L-PGA-VEGF 30:1 formulation was more rapid. There are many possible reasons for the more rapid release

observed with the L-PGA-VEGF 30:1 nanomedicine. Firstly, as previously stated the L-PGA has a much shorter half-life *in vivo* than its star-shaped counterpart [36]. Similarly, Byrne et al. found that even in the presence of the enzymes thermolysin and chymotrypsin release of rhodamine B from L-PGA was more rapid and complete than that observed with an 8 armed star-PGA similar to the one used in this work [23].

Silva et al. have previously observed *in vivo* VEGF release from an alginate gel containing 250 ng VEGF/ml of hydrogel of 60% over the first seven days followed by release of a further 20% up to day 28. The released VEGF significantly improved murine hindlimb perfusion [13]. Thus, the *in vitro* release profile from the star-PGA-VEGF nanomedicines, with most release occurring over the first seven days followed by release of small amounts of VEGF up to day 28 could potentially improve vessel formation *in vivo*. Less than 30% of the loaded VEGF was recovered overall during release studies. In light of a reported 90 minute half-life at 37°C this is neither surprising nor uncommon and has been reported previously in the literature [42]. Furthermore studies where such low recoveries of VEGF have been noted have gone on to be efficacious in inducing angiogenesis in animal models with no apparent associated toxicity [18, 32].

Star-PGA-VEGF 30:1 and 50:1 nanomedicines were capable of inducing significantly better tubule lengths at both 6 and 12 hours compared to cells alone. Furthermore, the increase in tubule length observed at 6 hours for both star-PGA-VEGF nanomedicines is as statistically significant as that seen for non-encapsulated VEGF at 6 hours. The star-PGA-VEGF nanomedicines have only released approximately 3.5 ng (30:1) and 1 ng (50:1) VEGF respectively, in comparison to the 50 ng in the control group. This greater effect may be due

to increased potency of the VEGF released which, unlike the VEGF in the control group, is possibly not being degraded and is protected inside the nanoparticle. Despite having released approximately 5 ng of VEGF by 6 hours, the L-PGA-VEGF formulation has less significant effects on tubule length with a significant increase in length only seen at 12 hours. This may be due to the possible toxic effects of the L-PGA molecule itself (Online Resource S4). Overall the results of this experiment indicate that the star-PGA-VEGF 30:1 and 50:1 formulations may be superior to their L-PGA-VEGF 30:1 counterpart. Vessel sprouting is one of the main processes involved in the initiation and progression of angiogenesis *in vivo* [30, 43]. Previously, VEGF induced microvessel formation *in vitro* has translated to improvements in *in vivo* vessel formation and density [17, 20].

As well as vessel formation assays, cell migration assays can also be of use in assessing the *in vivo* angiogenic potential of formulations [43, 44]. The star-PGA-VEGF 50:1 nanomedicines were capable of inducing significant migration producing gap closure at 24 hours. Neither the L-PGA-VEGF 30:1 nor the star-PGA-VEGF 30:1 nanomedicines were capable of achieving gap closure at 24 hours. Therefore, star-PGA-VEGF 50:1 nanomedicines were selected for further development. Overall the results obtained from this scratch assay are in line with those obtained by Anderson et al. with their Heparin-VEGF nanoparticles which achieved 60% gap closure at 18 hours and these particles went on to improve vessel formation in an *in vivo* assay [45].

The star-PGA-VEGF nanomedicines were then incorporated into a hydrogel in order to effectively deliver and retain the nanomedicines at the site of action. Hydrogels have shown promise in their own right for improving patient symptoms following an MI [27]. Hydrogels which can be injected through a catheter system may also aid minimally invasive delivery of

the nanomedicines. Hyaluronic acid is a molecule which has been in clinical use for over thirty years and its safety has been well established in both the pharmaceutical and cosmetic sectors [28]. Chemical crosslinking mechanisms mean that incorporation of cargo during the formulation process of these hydrogels is possible.

Star-PGA-VEGF 50:1 nanomedicines were incorporated into a HA-TA hydrogel. Rheology confirmed that hydrogel formation was still possible following inclusion of the PGA-VEGF nanomedicines in the hyaluronic acid dispersion. A higher G' was achieved in the absence of the star-PGA-VEGF 50:1 nanomedicines indicating some form of interaction between the PGA and the crosslinkers which are then impeded from forming the normal links within the hydrogel, lowering the storage modulus. The storage modulus observed here is within the range of moduli previously identified as suitable for endocardial delivery of hydrogels, with Algisyl® having a reported storage modulus of 3-5 kPa [27]. Injections of hydrogels into the heart have previously consisted of multiple injections around the site of damage [27]. Fig. 6(b) indicates that the fluorescently tagged star-PGA-VEGF 50:1 nanomedicines are evenly distributed in the hydrogel which confirms uniform mixing of the precursor dispersions.

VEGF release, both free and within star-PGA nanomedicines, from the HA-TA hydrogels was investigated. Free VEGF loaded into HA-TA was released rapidly with 17% recovered within 24 hours. No further VEGF release was recorded thereafter. In contrast, when the star-PGA-VEGF 50:1 nanomedicines were integrated into the hydrogel VEGF release was detected for up to 35 days. Overall, VEGF recovery was also higher from this system with 42% quantified over the release study period compared to 17% for free VEGF in the HA-TA system. Such differences in VEGF release when incorporated into a double matrix system have previously been reported in the literature. Des Rieux et al. reported 20% VEGF release over 14 days when

1 µg VEGF was incorporated into 500 µl Matrigel® compared to just 2% VEGF release when dextran-chitosan-VEGF nanoparticles were loaded into the Matrigel® [18].

Bioactivity of the VEGF released from the hydrogel systems was determined using a scratch assay and a Matrigel® assay. By day 14 the hydrogel containing non-encapsulated, 'free' VEGF had released 8.65 ng VEGF, while that containing the star-PGA-VEGF 50:1 nanomedicines had released 11.5 ng VEGF. Thus a dose of 10 ng free, fresh VEGF was chosen as an appropriate control. The results of the Matrigel® assay (Fig. 7(b)) show that the VEGF released from both preparations was capable of inducing increases in tubule length similar to those induced by control VEGF. This result is confirmed on the scratch assay where gap closure was achieved by 24 hours with VEGF released from PGA-VEGF-HA-TA. Overall the tubule formation exhibited by all groups in Fig. 7(a) is less than that seen in Fig. 4. This is reasonable due to the reduced VEGF dose used in this experiment to facilitate comparison with the amount of VEGF released from the hydrogel.

Taken together these results suggest the development of an innovative sustained delivery system for the angiogenic growth factor VEGF, which may overcome the current technical barriers to effective growth factor delivery to improve post-MI angiogenesis and reduce progression to heart failure.

Conclusion

In this paper we have successfully developed a sustained release nano-in gel system that facilitates sustained release of VEGF for use in cardiac applications.

A method for the effective loading of linear and star-PGA polypeptides with VEGF was developed which maintains the integrity of the growth factor and can be easily scaled-up. Both PGA architecture and formulation parameters (molar ratios of PGA:VEGF) were found to be critical in developing an effective controlled release and bioactive formulation for VEGF. Star-PGA-VEGF nanomedicines formulated at a PGA-VEGF ratio of 50:1 were found to provide sustained VEGF release while maintaining bioactivity post encapsulation. These PGA-VEGF 50:1 nanomedicines were successfully incorporated into a hyaluronic acid dispersion and gel formation occurred following injection through the BHM. Finally we report the formation of a bioactive, sustained release, double matrix system for the delivery of the angiogenic growth factor VEGF. This PGA-VEGF-HA-TA system maintains VEGF bioactivity and has favourable material and fabrication properties for scale-up, thus making it a prototype delivery platform system for other growth factors of interest, advancing the delivery of these labile cargoes and improving the lives of patients post-MI.

Acknowledgements:

The authors acknowledge the support of Brenton Cavanagh for assistance with imaging and Matrigel® analysis. This study was undertaken as part of the Translational Research in Nanomedical Devices (TREND) research project, School of Pharmacy, RCSI, facilitated via a Science Foundation Ireland Investigators Program 13/IA/1840.

Conflict of Interest Statement:

References

1. RN P. The Circulatory System and Oxygen Transport. In: Sciences MCL, editor. Regulation of Tissue Oxygenation San Rafael (CA)2011

2. Alberts B, Johnson A, J L. Blood Vessels and Endothelial Cells. In: Science G, editor. Molecular Biology of the Cell. New York2002.

3. Buja LM, Vander Heide RS. Pathobiology of Ischemic Heart Disease: Past, Present and Future. Cardiovascular Pathology. 2016;25(3):214-20.

4. O'Brien FJ. Biomaterials & scaffolds for tissue engineering. Materials Today. 2011;14(3):88-95.

5. Duffy GP, McFadden TM, Byrne EM, Gill S, FarrelL E, O'Brien FJ. Towards in vitro vascularisation of Collagen-GAG scaffolds. European Cells and Materials. 2011;21:15-30.

6. Shah AM, Mann DL. In Search of New Therapeutic Targets and Strategies for Heart Failure: Recent Advances In Basic Science. Lancet. 2011;378(9792):704-12.

7. Cochain C, Channon KM, Silvestre J-S. Angiogenesis in the Infarcted Myocardium. Antioxidants & Redox Signaling. 2013;18(9):1100-13.

8. Adair T, Montani J. Angiogenesis. In: Sciences MCL, editor. Overview of Angiogenesis. San Rafael (CA)2010.

9. Ferrara N, Henzel WJ. Pituitary follicular cells secrete a novel heparin-binding growth factor specific for vascular endothelial cells. Biochemical and Biophysical Research Communications. 1989;161(2):851-8.

10. Thomas K. Vascular Endothelial Growth Factor, a potent and selective angiogenic agent. The Journal of Biological Chemistry. 1996;271(2):603-6.

11. Henry TD, Rocha-Singh K, Isner JM, Kereiakes DJ, Giordano FJ, Simons M, et al. Intracoronary administration of recombinant human vascular endothelial growth factor to patients with coronary artery disease. Am Heart J. 2001;142(5):872-80.

12. Henry TD. The VIVA Trial: Vascular Endothelial Growth Factor in Ischemia for Vascular Angiogenesis. Circulation. 2003;107(10):1359-65.

13. Silva EA, Mooney DJ. Effects of VEGF temporal and spatial presentation on angiogenesis. Biomaterials. 2010;31(6):1235-41.

14. Panyam J, Labhasetwar V. Biodegradable nanoparticles for drug and gene delivery to cells and tissue. Advanced Drug Delivery Reviews. 2003;55(3):329-47.

15. Davda J, Labhasetwar V. Characterization of nanoparticle uptake by endothelial cells. International Journal of Pharmaceutics. 2002;233(1):51-9.

16. Golub JS, Kim Y, Duvall CL, Bellamkonda RV, Gupta D, Lin AS, et al. Sustained VEGF delivery via PLGA nanoparticles promotes vascular growth. Am J Physiol Heart Circ Physiol. 2010;298(6):H1959-65.

17. Xie J, Wang H, Wang Y, Ren F, Yi W, Zhao K, et al. Induction of angiogenesis by controlled delivery of vascular endothelial growth factor using nanoparticles. Cardiovasc Ther. 2013;31(3):e12-8.

18. des Rieux A, Ucakar B, Mupendwa BP, Colau D, Feron O, Carmeliet P, et al. 3D systems delivering VEGF to promote angiogenesis for tissue engineering. J Control Release. 2011;150(3):272-8.

19. Gu F, Amsden B, Neufeld R. Sustained delivery of vascular endothelial growth factor with alginate beads. J Control Release. 2004;96(3):463-72.

20. Oduk Y, Zhu W, Kannappan R, Zhao M, Borovjagin AV, Oparil S, et al. VEGF nanoparticles repair the heart after myocardial infarction. American Journal of Physiology-Heart and Circulatory Physiology. 2018;314(2):H278-H84.

21. Desai N. Challenges in Development of Nanoparticle-Based Therapeutics. The AAPS Journal. 2012;14(2):282-95.

22. Yan Y, Wei D, Li J, Zheng J, Shi G, Luo W, et al. A poly(l-lysine)-based hydrophilic star block co-polymer as a protein nanocarrier with facile encapsulation and pH-responsive release. Acta Biomaterialia. 2012;8(6):2113-20.

23. Byrne M, Thornton PD, Cryan S-A, Heise A. Star polypeptides by NCA polymerisation from dendritic initiators: synthesis and enzyme controlled payload release. Polymer Chemistry. 2012;3(10):2825.

24. Wang X, Wu X, Xing H, Zhang G, Shi Q, E L, et al. Porous Nanohydroxyapatite/Collagen Scaffolds Loading Insulin PLGA Particles for Restoration of Critical Size Bone Defect. ACS Applied Materials & Interfaces. 2017;9(13):11380-91.

25. Saludas L, Pascual-Gil S, Prosper F, Garbayo E, Blanco-Prieto M. Hydrogel based approaches for cardiac tissue engineering. Int J Pharm. 2017;523(2):454-75.

26. Van Vlierberghe S, Dubruel P, Schacht E. Biopolymer-based hydrogels as scaffolds for tissue engineering applications: a review. Biomacromolecules. 2011;12(5):1387-408.

27. Mann DL, Lee RJ, Coats AJ, Neagoe G, Dragomir D, Pusineri E, et al. One-year follow-up results from AUGMENT-HF: a multicentre randomized controlled clinical trial of the efficacy of left ventricular augmentation with Algisyl in the treatment of heart failure. Eur J Heart Fail. 2016;18(3):314-25.

28. Burdick JA, Prestwich GD. Hyaluronic acid hydrogels for biomedical applications. Adv Mater. 2011;23(12):H41-56.

29. Tahergorabi Z, Khazaei M. A Review on Angiogenesis and Its Assays. Iranian Journal of Basic Medical Sciences. 2012;15(6):1110-26.

30. Auerbach R, Lewis R, Shinners B, Kubai L, Akhtar N. Angiogenesis Assays: A Critical Overview. Clinical Chemistry. 2003;49(1):32-40.

31. Arnaoutova I, Kleinman HK. In vitro angiogenesis: endothelial cell tube formation on gelled basement membrane extract. Nat Protoc. 2010;5(4):628-35.

32. Quinlan E, Lopez-Noriega A, Thompson EM, Hibbitts A, Cryan SA, O'Brien FJ. Controlled release of vascular endothelial growth factor from spray-dried alginate microparticles in collagen-hydroxyapatite scaffolds for promoting vascularization and bone repair. J Tissue Eng Regen Med. 2015.

33. Lee K, Silva EA, Mooney DJ. Growth factor delivery-based tissue engineering: general approaches and a review of recent developments. J R Soc Interface. 2011;8(55):153-70.

34. Taraballi F, Pandolfi L, Powell S, Cabrera FJ, A T, Minardi S, et al. Strategic Approaches to Growth Factors Delivery for Regenerative Medicine

In: Panseri S, Taraballi F, Cunha C, editors. Biomimetic Approaches for Tissue Healing: OMICS Group; 2015.

35. Rodell CB, Lee ME, Wang H, Takebayashi S, Takayama T, Kawamura T, et al. Injectable Shear-Thinning Hydrogels for Minimally Invasive Delivery to Infarcted Myocardium to Limit Left Ventricular Remodeling. Circ Cardiovasc Interv. 2016;9(10).

36. Duro-Castano A, England RM, Razola D, Romero E, Oteo-Vives M, Morcillo MA, et al. Well-Defined Star-Shaped Polyglutamates with Improved Pharmacokinetic Profiles As Excellent Candidates for Biomedical Applications. Molecular Pharmaceutics. 2015;12(10):3639-49.

37. Anderson W, Kozak D, Coleman VA, Jamting AK, Trau M. A comparative study of submicron particle sizing platforms: accuracy, precision and resolution analysis of polydisperse particle size distributions. J Colloid Interface Sci. 2013;405:322-30.

38. Filipe V, Hawe A, Jiskoot W. Critical evaluation of Nanoparticle Tracking Analysis (NTA) by NanoSight for the measurement of nanoparticles and protein aggregates. Pharm Res. 2010;27(5):796-810.

39. Walsh DP, Murphy RD, Panarella A, Raftery RM, Cavanagh B, Simpson JC, et al. Bioinspired Star-Shaped Poly(l-lysine) Polypeptides: Efficient Polymeric Nanocarriers for the Delivery of DNA to Mesenchymal Stem Cells. Molecular Pharmaceutics. 2018.

40. Kita K, Dittrich C. Drug delivery vehicles with improved encapsulation efficiency: taking advantage of specific drug–carrier interactions. Expert Opinion on Drug Delivery. 2011;8(3):329-42.

41. Rui J, Dadsetan M, Runge MB, Spinner RJ, Yaszemski MJ, Windebank AJ, et al. Controlled release of vascular endothelial growth factor using poly-lactic-co-glycolic acid microspheres: In vitro characterization and application in polycaprolactone fumarate nerve conduits. Acta biomaterialia. 2012;8(2):511-8.

42. Kleinheinz J, Jung S, Wermker K, Fischer C, Joos U. Release kinetics of VEGF(165)from a collagen matrix and structural matrix changes in a circulation model. Head & Face Medicine. 2010;6:17-.

43. Staton CA, Reed MW, Brown NJ. A critical analysis of current in vitro and in vivo angiogenesis assays. Int J Exp Pathol. 2009;90(3):195-221.

44. Liang CC, Park AY, Guan JL. In vitro scratch assay: a convenient and inexpensive method for analysis of cell migration in vitro. Nat Protoc. 2007;2(2):329-33.

45. Anderson SM, Siegman SN, Segura T. The effect of vascular endothelial growth factor (VEGF) presentation within fibrin matrices on endothelial cell branching. Biomaterials. 2011;32(30):7432-43.

Online Resources

Online Resource 1

Gel permeation chromatograms for L-PGA and star-PGA

Size exclusion chromatography was used to determine the dispersities ($Đ_M$) and molecular weights of the L-PGA and star-PGA polypeptides. SEC was conducted in 1,1,1,3,3,3-Hexafluoro-2-propanol (HFiP) using an PSS SECurity GPC system equipped with a PFG 7 µm 8 × 50 mm pre-column, a PSS 100 Å, 7 µm 8 × 300 mm and a PSS 1000 Å, 7 µm 8 × 300 mm column in series and a differential refractive index detector at a flow rate of 1.0 ml min^{-1}. The systems were calibrated against Agilent Easi-Vial linear poly(methyl methacrylate) (PMMA) standards and analysed by the software package PSS winGPC UniChrom.

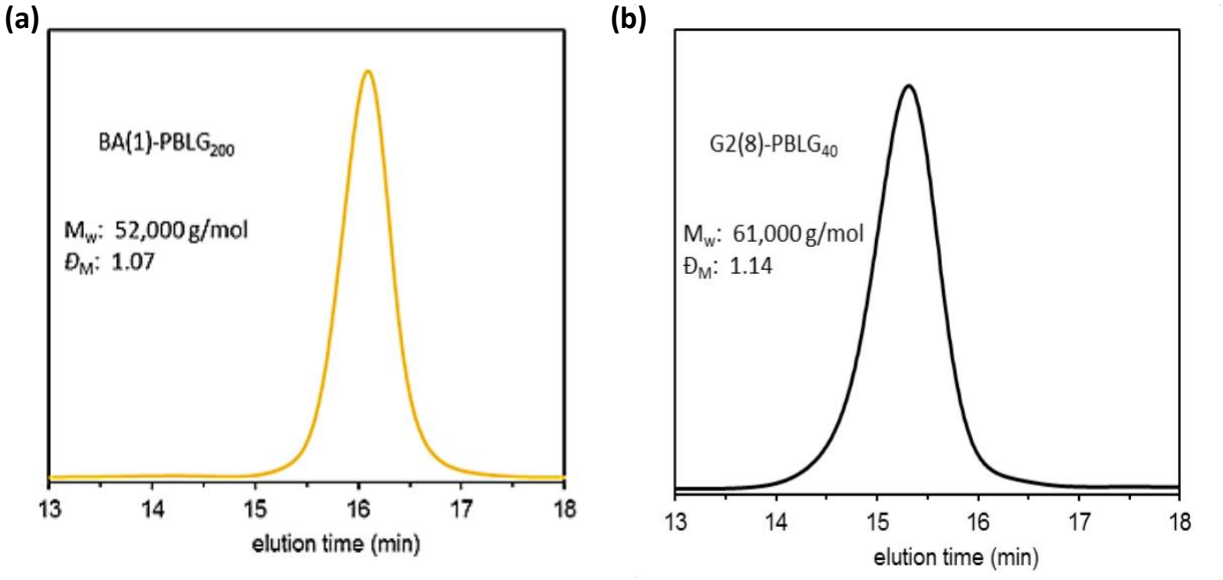

S1 (a) Gel permeation chromatography (GPC) output for Benzylamine (BA)-Poly-benzyl-L-glutamate. Deprotection of this molecule results in the formation of L-PGA **(b)** GPC output for G2(8)-PBLG$_{40}$. Deprotection of this molecule results in the formation of star-PGA.

Online Resource 2

Determination of optimal complexation procedure

Complexation time and temperature were varied to identify the optimal complexation procedure. Particles complexed in the fridge had a larger Z-average size than those complexed at room temperature. 5 minutes complexation was determined to be a more practical complexation time for particle manufacture and nano-sized complexes formed in this time period. Thus, 5 minutes complexation at room temperature was defined as the optimal complexation procedure. Star-PGA:VEGF ratios of 10:1 or 20:1 either did not form particles reproducibly or formed particles with a large PDI. Thus, these were omitted from further studies. Star-PGA:VEGF ratios of 100:1 and 200:1 did not have a significantly better PDI than the star-PGA-VEGF 50:1 formulations, thus these were also omitted from further studies as there was no justification for the use of the higher star-PGA dose in these formulations. Mimicking the bracketing procedure often used in the pharmaceutical industry the star-PGA-VEGF 30:1 and 50:1 formulations were chosen for further studies.

S2 Z-average size (Z-ave), Zeta potential (ZP) and polydispersity index (PDI) of star-PGA-VEGF dispersions at various star-PGA:VEGF ratios and complexation conditions. n=3.

Star-PGA:VEGF Ratio	Complexation time: 5 minutes			Complexation time: 30 minutes		
	Z-ave (nm)	ZP (meV)	PDI	Z-ave (nm)	ZP (meV)	PDI
Complexation in the Fridge						
10:1				1796	-2.7	0.6
20:1	690.8	-4	0.6	710	-9.7	0.4
30:1	741.2	-3.2	0.4	444.5	-1.7	0.3
40:1	749.1	-4.7	0.3	399.6	-2.8	0.3
50:1	428.1	-2.1	0.3	639.1	-3.8	0.6
100:1	318.8	-2.7	0.6	422	-3	0.4
200:1	360.4	-4.9	0.3	382.9	-5.3	0.5
Complexation at Room Temperature						
10:1	828.9	-3.6	0.4	363.2	-1.5	0.4
20:1	545.6	-5.4	0.5	601.3	-3.9	0.3
30:1	444.5	-2.3	0.3	568.1	-2.6	0.4
40:1	505.5	-3.2	0.3	835	-2.3	0.3
50:1	415.5	-3.6	0.2	433.6	-2.4	0.3
100:1	333.7	-2.9	0.4	407.7	-10.1	0.3
200:1	417.6	-5	0.5	334.5	-4.6	0.4

S3 Z-average size (Z-ave), Zeta potential (ZP) and polydispersity index (PDI) of L-PGA-VEGF dispersions. The L-PGA:VEGF ratio corresponds to the star-PGA:VEGF ratio with the same amount of glutamic acid units:VEGF. n=3.

L-PGA-VEGF ratio	**5 minutes complexation at room temperature**		
	Z-ave (nm)	**ZP (meV)**	**PDI**
20:1	539.1	-2.1	0.6
30:1	656.7	-7.7	0.4
40:1	660.9	-7.5	0.5
50:1	406.2	-7.9	0.4
100:1	753.4	-3.9	0.3
200:1	352.7	-8.8	0.3

Online Resource 3

Biocompatibility of developed star-PGA-VEGF and L-PGA-VEGF nanomedicines

Toxicity of the nanomedicines was tested to ensure their suitability for biomedical applications. Live/Dead Cell Viability Staining was used to examine the biocompatibility of the formed nanoparticles. HUVECs at P4 were seeded in a 24 well Corning® Costar® tissue culture plate at a seeding density of 3 x 10^4 cells per well. Cells were given fully supplemented endothelial medium for 24 hours. This medium was then removed and replaced with either medium containing all supplements except VEGF (cells alone group), medium containing non-encapsulated VEGF at a concentration of 50 ng/ml or medium containing no non-encapsulated VEGF but containing the PGA-VEGF nanomedicines (VEGF 50 ng/ml). At the selected time points: 4, 24, 48 and 72 hours, the medium was removed and the cells were washed three times with PBS. 100 µl of live/dead solution (2 µM calcein AM, 4 µM ethidium homodimer) was then added to the well and left to incubate for 15 minutes protected from light at room temperature. Wells were imaged using a fluorescent microscope (Leica Microsystems, Switzerland) and Live and Dead images were merged using ImageJ software.

As a further assessment of the toxicity of the linear and star-PGA-VEGF nanomedicines metabolic activity of HUVECs exposed to linear PGA-VEGF 30:1, star-PGA-VEGF 30:1 or star-PGA-VEGF 50:1 was measured. The procedure for the experiment was the same as that outlined above except that at the selected time points of 4, 24, 48 and 72 hours, medium was removed and 100 µl of CellTiter 96® Aqueous One Solution Cell Proliferation Assay (MTS) was added to each well. The plate was incubated at 37°C for three hours. Absorbance was measured on a Varioskan plate reader at 490 nm. Metabolic activity in each of the treatment groups was normalised to that of the cells alone group at each time point.

At all time points cells exposed to VEGF free medium or medium supplemented with 50 ng/ml non-encapsulated VEGF appeared to be alive and growing. The most dead cells observed were in the wells containing L-PGA-VEGF 30:1 nanomedicines and cell number also appeared lowest in this group.

Corresponding to the data obtained with the Live/Dead staining the star-PGA:VEGF 30:1 and 50:1 nanomedicines appeared to be biocompatible. The L-PGA-VEGF 30:1 nanomedicines showed significant toxicity at the 4 hour and 72 hour time points.

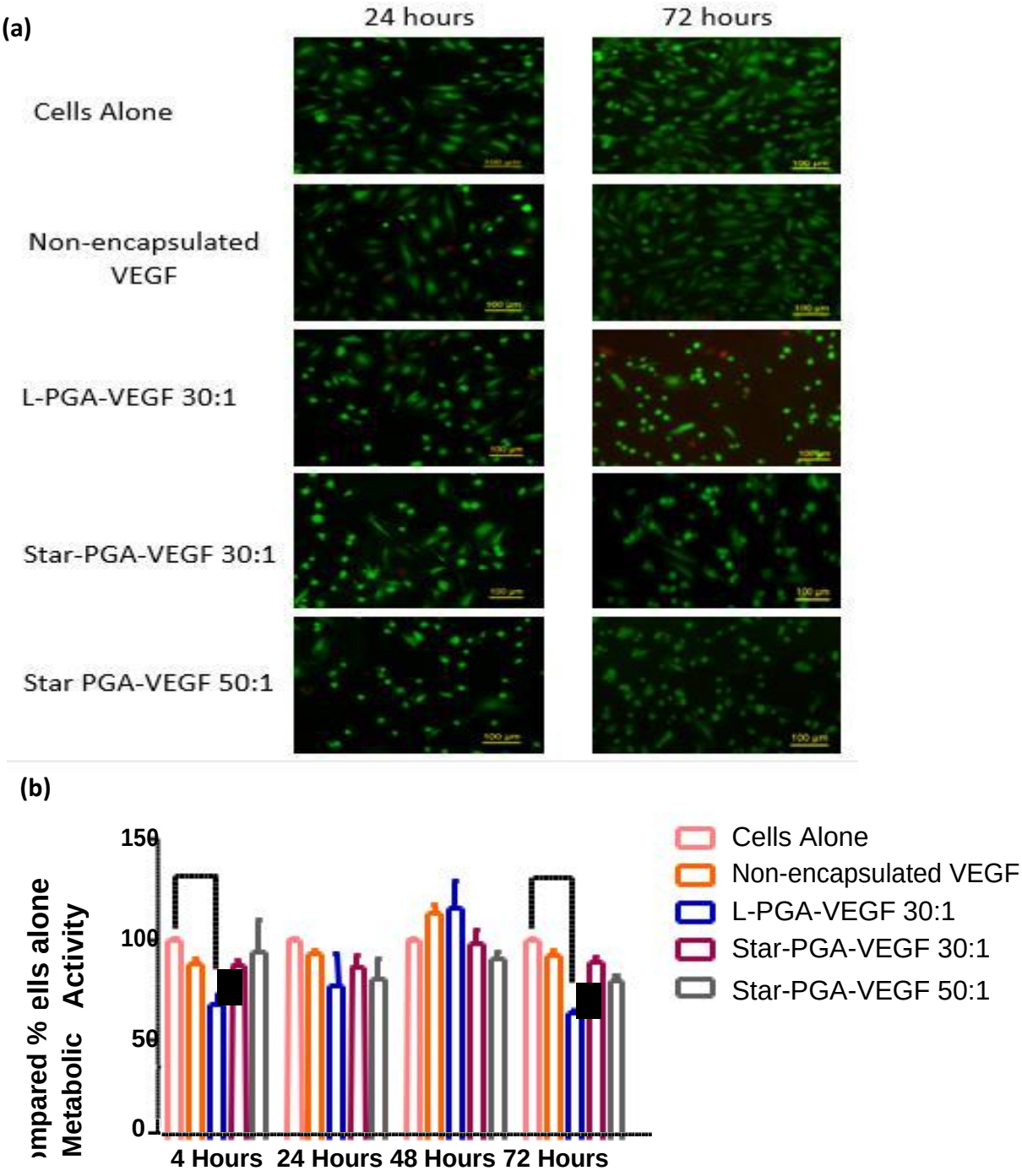

S4 (a) Images obtained from Live/Dead staining of HUVECs following treatment with PGA-VEGF nanomedicines **(b)** Metabolic activity of cells in the presence of PGA-VEGF nanomedicines compared to that of untreated, healthy cells. VEGF concentration in each group: 50 ng/ml. n=3; **p<0.01.